Infectivity of Human Olfactory Neurons to SARS-CoV-2: A Link to Anosmia

Omar Bagasra[1*], Pratima Pandey[1], Jessica R. Sanamandra, Jarrett M. Houston, Ewen McLean[2] and Helmut Albrecht[3]

[1]Claflin University, South Carolina Center for Biotechnology, 400 Magnolia Street, 29115 Orangeburg, SC, United States.
[2]Aqua Cognoscenti LLC, West Columbia, SC 29170, USA.
[3]Department of Internal Medicine, PRISMA Health Midlands, University of South Carolina, Columbia, SC.

Received: 26 March 2021
Accepted: 26 July 2021

*Corresponding Author: obagasra@claflin.edu

DOI 10.5001/omj.2021.128

Abstract

To determine whether SARS-CoV-2 infections are associated with anosmia and does this virus infect other neuronal cells we utilized male and female olfactory neuronal cell lines as well other olfactory cells lines to determine the viral targets. Therefore, we utilized four undifferentiated and two partially differentiated human developing neuronal cell lines. Infectivity was confirmed by RT-qPCR, immunofluorescence assay (IFA) probing with anti-SARS-CoV-2 antibody, evaluation of cytopathic effects and neurite formation. Since both olfactory cell lines were terminally differentiated, we induced partial differentiation of all cell lines with retinoic acid (RA) to determine whether differentiation was a factor in viral permissiveness. The expression of serine protease, transmembrane serine protease 2 (TMPRSS2), and angiotensin-converting enzyme II (ACE2) receptors were examined by RT-qPCR and IFA to determine the mechanism of viral entry. Four-to-five days after exposure both olfactory cell lines exhibited morphological evidence of infection; IFA analyses indicated that ~30% of the neurons were SARS-CoV-2 positive. At 2 weeks, 70-80% were positive for SARS-CoV-2 antigens. The partially differentiated (CRL-2266 and CRL-2267) and undifferentiated cell lines (CRL 2142 CRL 2149, CRL-127 and CDL-2271) were essentially non-permissive. After RA treatment only CRL-127 exhibited slight permissiveness (RT-qPCR). The TMPRSS2 receptor showed high expression in olfactory neurons but low expression in RA treated CRL-127. ACE2 expression by RT exhibited high expression in olfactory neurons whereas other cell lines showed low expression including RA-treated cell lines. ACE2 expression slightly increased in CRL-127 post RA-treatment. Our studies confirm neurotropism of SARS-CoV-2 to olfactory neurons with viral entry likely mediated by TMPRSS2/ACE2. Other neuronal cell lines were non-permissive.

Lay summary: We examined whether nerve cells involved in smell and taste could be infected by the COVID-19 virus. To see if there were gender differences, we used cells from both

males and females and exposed them to the virus. Viral infection was confirmed using various methods. Our results established that the nerve cells were infected regardless of male or female origin and strengthened the reported association of COVID-19 with loss of smell in infected individuals.

Key Words: ACE2, Anosmia; Axon; differentiated; Neurogenesis; Neuroblastoma; neurite formation; retinoic acid; SARS-CoV-2 virus; TMPRSS2; Undifferentiated.

Introduction

When compared against the mortality rates estimated for the 1918-1920 H1N1 influenza A pandemic, the current deaths caused by COVID-19 are only slight. The so-called Spanish 'flu pandemic, which came in three to four waves, between March 1918 and February 1920, is estimated to have accounted for a low of around 18 million deaths (Spreeuwenberg et al., 2018), or 1% of the then global population, to a high of 100 million mortalities (Johnson and Mueller, 2002), or 5.6% of the population. In contrast, the present pandemic, caused by SARS-CoV-2 (CSGICTV, 2020), is presently credited with approximately 2.6 million deaths or about 0.3% of the global population. Nonetheless, the current public health emergency caused by SARS-CoV-2, has led many governments to institute strict quarantine measures to prevent its spread. Use of personal protective clothing, physical distancing, prohibition of gatherings, lockdowns and curfews have all become familiar policies in efforts to curtail viral infection rates and mortality.

Like the Spanish 'flu, the SARS-CoV-2 virus has been associated with a variety of symptoms including, but not limited to, acute respiratory distress (ARDS), which has been one of the major causes of death (Rothan and Byrareddy, 2020), dizziness and headache, sore throat, muscle fatigue and fever, nausea, diarrhea, and vomiting (CDC, 2021). Well-documented effects of H1N1 were inflammation of the optic nerve, blurred, and impaired color vision (Spinney, 2018) and recent reports suggest that SARS-CoV-2 equally impacts the optic nerve

(Burgos-Blasco et al., 2020). Another similarity between SARS-CoV-2 and H1N1 is its impact on taste and smell. Indeed, it appears that one of the earliest and more specific symptoms of SARS-CoV-2 infection is development of anosmia. In many cases, loss of smell and taste are noticed earlier than other symptoms, with patients otherwise remaining asymptomatic and recovering from the virus (Lechien et al., 2020; Meng et al., 2020).

A number of possible causes underlying the development of anosmia during SARS-CoV-2 infection have been proposed. These include straightforward triggers, such as nasal blockage and rhinorrhea, perhaps coupled with olfactory cleft syndrome and cytokine release syndrome, through to disruption of olfactory receptor neurons and injury to olfactory perception centers in the brain (Klopfenstein et al., 2020; Bilinska and Butowt, 2020;). Here we explore potential mechanisms of anosmia at cellular and molecular levels using both male and female olfactory neuronal cell lines, and four undifferentiated, and two partially differentiated human developing neuronal cell lines. Since the olfactory system is unique among sensory systems that is constantly going through neurogenesis throughout life and its primary differentiated neurons bi-polar neurons come direct in contact with the external environment, we examine whether differentiation is a factor determining viral permissiveness. Of note, the olfactory bulb is a six-layer structure in which the sequential stages of odor information processing take place. The axons on the cilia of olfactory receptor neurons (ORNs) in the nasal olfactory mucosa form the olfactory nerve layer of the OB [Bilinska & Butowt, 2020]. Secondary olfactory neurons, known as mitral cells (MCs) located in the mitral cell layer of OB, and tufted cells (TCs) located in the external plexiform layer, all innervate OB glomeruli. In addition, a large number of granule axon-less interneurons are located in the most central cell layer of the OB. The apical dendrites of

granule cells form synapsis with MCs and TCs. The expression of serine protease, transmembrane serine protease 2 (TMPRSS2), and angiotensin-converting enzyme II (ACE2) receptors were also examined to evaluate potential mechanisms of viral entry.

Materials and methods

Reagents and Cell Lines: Six undifferentiated human neuroblastoma (NB) cell lines were purchased from ATCC (New York, NY). CRL-2267, CCL-127, CRL-2271 (of male origin) CRL-2266, and CRL- 2149, (of female origin) were cultured in Eagle's Minimum Essential Media (EMEM) (ATCC, Manassas, VA) supplemented with 10% heat inactivated Fetal Bovine Serum (FBS), and L-Glutamine-penicillin-streptomycin solution (designated complete media) (Sigma, St. Louis, MO) at 37^{o}C, 5% CO_2.Two olfactory NB cell lines, TC-268 and JFEN, of female and male origin, respectively, were a kind gift from Timothy J. Triche (Department of Pathology, Children's Hospital of Los Angeles, Los Angeles, CA 90027). The stock cell cultures were grown in 25 mL or 75 mL flasks (Thermo-Scientific, Nunc, Rochester, NY). Three SARS-CoV-2 isolates were collected from confirmed SARS-CoV-2 infected individuals; one isolate was used for the initial studies (Hughes et al., 2016). HT29mer, a colon epithelial cell line (William G. Thilly, Biological Engineering, MIT) was used as a negative control.

Propagation of SARS-CoV-2: Each of the three SARS-CoV-2 samples were propagated in Vero cells (ATCC). The cells were grown in EMEM at 80% confluency in 25 mL tissue culture flasks (Nunc Inc., USA). Following removal of the culture media, viral inoculum was added to give a Multiplicity of Infection (MOI) of 0.1 to 0.05/cell. Flasks were incubated at 37^{o}C, 5% CO_2 with gentle agitation for 2 hrs. After incubation, the unattached virions were removed by gentle washing with 5 mL of PBS and then 5 mL of complete media was added,

and the cells were maintained for 5 days. Cells were trypsinized and cryopreserved in 1 mL vials in 50% FBS and 10% DMSO at -80^{o} C and used in subsequent studies (Hughes et al., 2016).

Infection of NB Cell Lines with SARS-CoV-2: To examine the permissiveness of NB cell lines to SARS-CoV-2, all 6 undifferentiated cell lines and two olfactory NB cell lines, TC-268 and JFEN (Hughes et al., 2016), were either grown in 25 mL tissue culture flasks or 8-well chamber slides (Thermo Scientific, Nunc, Rochester, NY) to ~60% confluency, media was removed and immediately exposed to an MOI of 0.1-0.05 in 1.0 mL serum free media. For maximum infectivity, the flasks were intermittently gently agitated for 2 h, washed once in 5mL PBS and then 5 mL of pre-warmed media was added. Control cultures were treated identically, except no SARS-CoV-2 was added to the 8-well chambers. The cells were incubated at 37^{o}C, 5% CO_2. The cell cultures remained in the 8-well chambers for 5-days and then the supernatants were carefully removed, and cells fixed in 2% fresh paraformaldehyde and the slides subsequently incubated under UV-light overnight in a SterilGuard BLS-2 hood (Baker Company). These slides were used to carry out IFA analyses. A separate set was stained with H & E for morphological analyses and images recorded on a digital camera (Olympus BX51). Each experiment was repeated at least three times. All experiments were carried out in a high containment laboratory according to the CDC guidelines for COVID-19 handling and all biosafety measures were taken to avoid the viral infection (CDC 2020).

Immunofluorescence Assay (IFA): For immunocytochemical studies, each cell line was grown in 8-well chamber slides with ~1x10^{5} cells in 0.3 µL of media for 5-days. For seeding the NB cell lines, the stock cell cultures, grown in the flasks, were gently washed once with

1x sterile phosphate buffered saline (PBS) (Fisher Scientific, Fair Lawn, NJ), followed by trypsinization, until single cell suspension and inactivation of trypsin with 1ml FBS. The cells were counted using a hemocytometer chamber and adjusted to $1x10^5$ cells/mL. The 8-well chamber slides were labeled, and 100 µL of cells added to each well together with 5 µL of fresh media containing 0.1-0.05 MOI of the virus. After 2 h incubation the cells were washed gently with pre-warmed PBS and 500 µL of fresh media added. After 5-days culture, the media was removed from the slides and the cells were fixed by adding 800 µL of 2% PFA to each well and allowed to set overnight at room temperature, under UV-light, in a SterilGuard Hood. The wells were then washed gently three times using 1x sterile PBS and then soaked with the blocking agent (containing 2% Bovine Serum Albumin (BSA) in 1x PBS) for 10 minutes. SARS-CoV-2 was detected by utilizing polyclonal nucleoprotein antibody to SARS-CoV-2 raised in rabbit (Cat #PA5-81794, Thermo-Fisher Scientific). All antibody dilutions were carried out in 2% BSA in 1x PBS. The primary Ab was diluted to 1:100 in blocking buffer. In each chamber, 100 µL of diluted primary Ab was added to each well. The slides were incubated at 4 ^{0}C overnight in a humidified chamber and then washed three times in 1x PBS. Then, goat anti-rabbit fluorescein conjugated secondary Ab was used at a working dilution of 1:40 with 100 µL in each well. The slides were incubated for 1 h at 37^{o}C in humidified chambers and then washed three times with PBS with 10 minutes incubation each time. The tops of the 8-well chamber were removed with a device provided by the manufacturer, without disturbing the fixed cells. The cells were washed in PBS three times and then mounted with glass coverslips using a drop of mounting solution containing 50% glycerol and 50% PBS. The slides were observed at resolutions of 10x, 40x, and 1000x

(with oil) using an Olympus BX51 fluorescent microscope. Each experiment was repeated at least 3 times. The slides were analyzed independently in a blind fashion by two observers.

Hematoxylin and Eosin (H &E) Staining: For morphological studies, each cell line was grown in 8-well glass chamber slides with 1×10^5 cells in 100 mL of media for five days, as described above. After five days, the media was removed from the slides, and the cells were fixed by adding 500 µL of freshly prepared 2% paraformaldehyde (PFA) to each well and allowed to incubate overnight at room temperature. The caskets of the glass slides were removed by the device provided by the manufacturer, and the slides were washed gently three times using 1× PBS. These slides were stained with freshly prepared H&E (Leica Biosystems Richmond, Inc., Richmond, IL), washed in distilled water for one minute, and mounted with the mounting buffer containing 50% PBS and 50% glycerol. These slides were observed under 10X and 40X magnification and analyzed for neurite formation, i.e., central chromatolysis, axonal length, thickness, thinning, and degeneration. Additionally, syncytia formation and other morphological and cytotoxic changes were recorded for comparing to controls. The experiments were repeated at least three times and the observations were recorded using a digital camera (Olympus BX51).

Qualitative Real-time PCR (RT-qPCR): The SARS-CoV-2 RNA copies were quantified using one-step RT-PCR. Viral RNA was extracted from culture pellets using GenElute Mammalian Total RNA Miniprep kit (Sigma, St. Louis, MO) according to the manufacturer's protocol. Two sets of primer pairs were designed to target the nucleocapsid region of the virus genome, according to CDC published primers (https://www.cdc.gov/coronavirus/2019-ncov/lab/rt-pcr-panel-primer-probes.html). The list of the primers for SARS-CoV-2, TMPRSS2 and ACE2 expression are listed in Table 1. The reactions of RT-qPCR were

carried out using an iScript One-step RT-PCR kit with SYBR Green (Bio-Rad, Hercules, CA) and quantification was performed using an ABI 7500 real-time cycler (Applied Biosystems, Foster City, CA). The thermal cycling profile of this assay consisted of a 15 min cDNA synthesis step at 50ºC, 5 min of iScript reverse transcriptase inactivation at 95ºC, followed by 40 cycles of PCR at 95ºC for 10 sec and a step of a single fluorescence emission data collection at 55°C for 30 sec. Each experiment was repeated three times. Results were analyzed using HID Real-Time PCR Analysis Software v1.2 (Thermo Scientific, Waltham, MA). The relative degree of SARS-CoV-2 replications in different cell lines were calculated using cycle threshold values (C_t).

Table 1

TMPRSS2_Primers

Primer 1	F:	5'-CAAGATGAGCCCACGCGTCCCTCAGCAGGATTG-3'
	R:	5' CCTCTTCCACATTTGACTTCAGATGATGTTGATAAAG-3'

SARS-CoV-2_Primers

Primer 1	F:	5'-TTACAACATTGGCCGCAAA-3'
	R:	5'-GCGCGACATTCCGAAGAA -3'
Primer 2	F:	5'-GGGAGCCTTGAATAGCAGCATTG -3'
	R:	5'-TGTAGCACGATTGCAGCATTG -3'

ACE2 Primers

Primer 1	F:	5'-GGGATCAGAGATCGGAAGAAGAAA-3'
	R:	3'-AGGAGGTCTGAACATCATCAGTG-5'

Primer 2	F:	5’-AAACATACTGTGACCCCGCAT-3’
	R:	3’-CCAAGCCTCAGCATATTGAACA-5’
Primer 3	F:	5’-TCCAGACTCCGATCATCAAGC-3’
	R:	3’-GCTCATGGTGTTCAGAATTGTGT-5’

Results

Real-Time PCR and Immunofluorescence Assay: To determine permissiveness of SARS-COV-2 infection in various cell lines, a presence/absence assay was conducted by RT-qPCR. Analysis for presence of SARS-COV-2 showed positive infection of olfactory cell lines only (arrows). The six undifferentiated human developing brain cell lines showed negative results (Table 2). The same uninfected cell lines were used as controls, which showed an absence of SARS-COV-2 RNA (Table 2). Similar to the controls, cell lines CRL-2266, CRL-2267, CRL-2271, CRL-2142, and CCL-127, were negative for SARS-COV-2 infection as determined by RT-qPCR. There were no differences in the degree of permissiveness of SARS-COV-2 between NB cell lines of male and female origin (Table 2). An immunofluorescence assay, with polyclonal nucleoprotein antibody to SARS-CoV-2, confirmed the RT-qPCR results (Table 2 and Fig. 1). All 8 cell lines were exposed to RA at 1mg/mL for 48 hrs to induce partial differentiation and exposed to SARS-CoV-2. After 48 hrs. of exposure to RA TC-268, JFEN and CRL-127 exhibited RA-induced cytotoxicity resulting in neuronal death as well as dysregulation in neurite formation: chromatolysis, elongation of axon, appearance of axon outside of axonal hillocks, and appearance of multiple axons. CRL-127 exhibited a low degree of permissiveness to the virus as determined

by IFA and RT-qPCR. Other cell lines: CRL-2266, CRL-2267, CRL-2142, CRL-2149 and CRL-2271 were partially differentiated via 48 h RA exposure, however, RA-exposure did not result in permissiveness to the virus in any cell lines as determined by RT-qPCR and IFA. The most prominent partial differentiation was observed in CRL-2266 and CRL-2267, where 38% and 29% of the neurons developed long axons and the neurons became highly elongated. However, neither of the cell lines became permissive to SARS-CoV-2. The presence or absence of SARS-COV-2 in all the cell lines was further confirmed by utilization of two sets of primer pairs by RT-qPCR and IFA. Both CRL-2142 and CRL-2149 exhibited low degree of non-specific binding. HT29mer (ATCC HTB-38) was negative for SARS-CoV-2.

Table 2

Cell line	IFA: SARS-CoV-2	RT-PCR	TMPRSS2 Receptor	ACH2 Receptors	Remarks
JFEN	33.67%	4+@	+++	+++	Differentiated neurons
TC-268	41.31%	4+@	+++	+++	Differentiated neurons
CRL-2266	-	-	-	+	progenitor neurons
CRL-2267	-	-	-	+	progenitor neurons
CRL-2142	-	-	-	+	progenitor neurons
CRL-2149	-	-	-	+	progenitor neurons
CRL-127	Rare*	-	+	+	progenitor neurons
CRL-2271	-	-	-	+	progenitor neurons
JFEN RA^	49.3%		+++	+	Differentiated neurons, RA-induced cytotoxicity and neurite deformation, RA-induced cytotoxicity.
TC-268 RA	62.5%		+++	+	Differentiated neurons, RA-induced cytotoxicity and neurite deformation. RA-induced cytotoxicity.
CRL-2266-RA	-	-	-	+	Partially differentiated with ~31% of cells with long axons
CRL-2267-RA	-	-	-	+	Partially differentiated with ~22% of cells with long axons
CRL-2142-RA	-	-	-	+	Partially differentiation with elongations of axons and neurite deformation.
CRL-2149-RA	-	-	-	+	Partially differentiation with elongations of axons and neurite deformation.

CRL-127-RA	<0.01%	+	++	++	Partially differentiated with ~32%% of cells with long axons. RA-induced cytotoxicity.
CRL-2271-RA	Rare	-	-	++	Partially differentiation with elongations of axons and neurite deformation.
HT-29mes	-	-	-	-	Human colon cancer epithelial cell line (negative control)

4+[@] is designated when the amplification line on gel band is very bright.

^ Treatment with retinoic acid (1 μg/mL) for 48 hours.

*Rare is designated when the band on the gel is clearly negative, similar to negative control, but IFA shows rare (~1:1,000) cells exhibit cytoplasmic positive cells for SARS-CoV-2 spike antigen. There were no apparent morphological changes, and no clear neurite deformation can be discerned between the controls and the infected cell lines.

Viral Entry Receptors: The permissiveness of the all the 8-cell lines were further explored by determining the expression of TMPRSS2 and ACE2 receptors. As shown in Table 2, the high permissiveness of TC-268 and JFEN correlated with high expression of TMPRSS2 and ACE2 receptors. Both olfactory cell lines demonstrated a relatively high degree of TMPRSS2 and ACE2 expression, whereas the other cells showed negative expression of the TMPRSS2 receptor, except for CRL-127. After RA-induced differentiation, only CRL-127 exhibited low expression of TMPRSS2, which correlated with RT-qPCR and IFA observations (Figs 1 and 2). Real time PCR for ACE2 receptors exhibited very low expression in all the non-olfactory neuronal cell lines. Except for JFEN and TC-269 cell lines, none of the other cell lines were permissive to the virus. Only, partially differentiated CRL-127 exhibited permissiveness, which correlated with the higher expression of TMPRSS2 and ACE2 receptors.

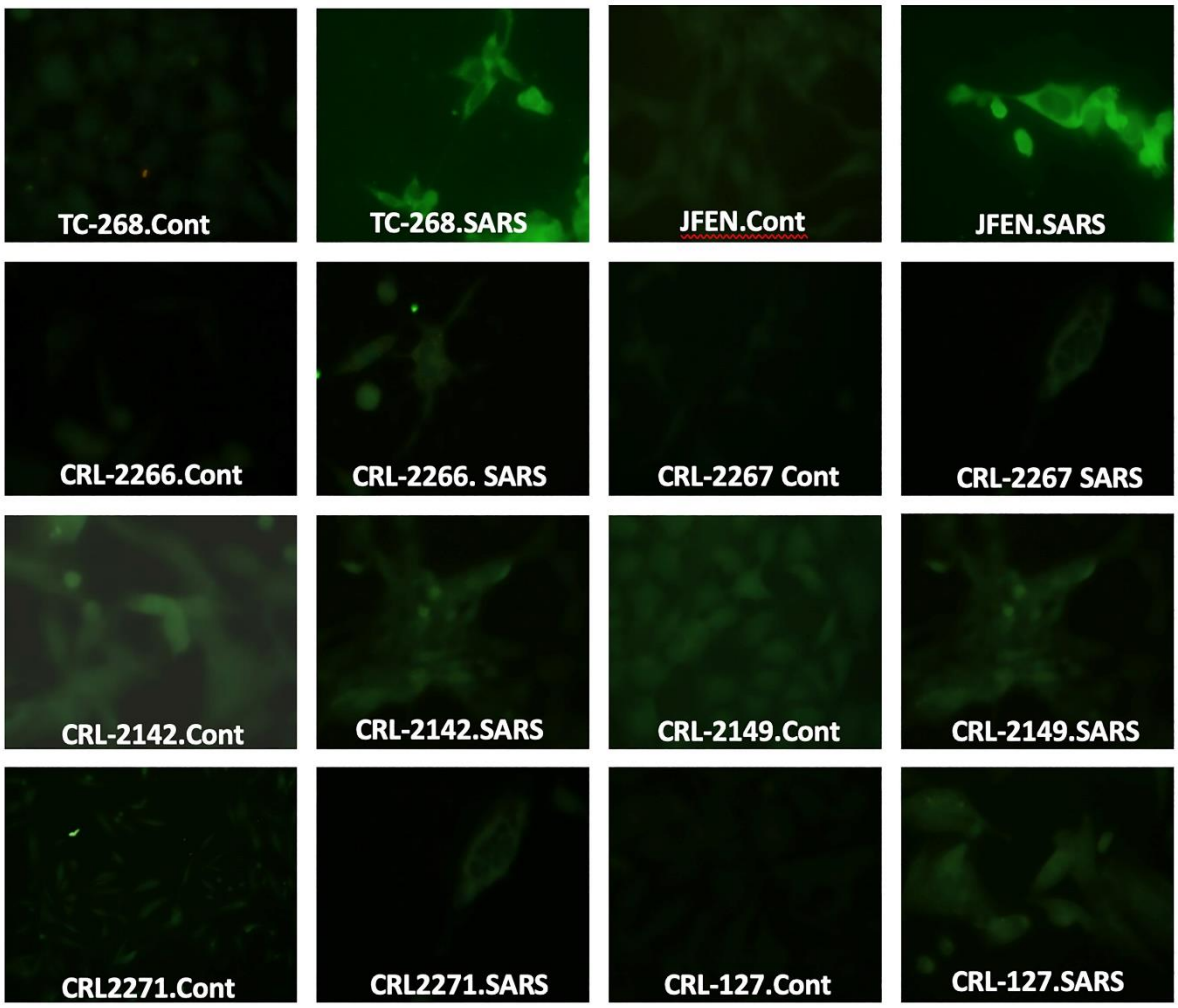
TC-268.Cont
TC-268.SARS
JFEN.Cont
JFEN.SARS
CRL-2266.Cont
CRL-2266. SARS
CRL-2267 Cont
CRL-2267 SARS
CRL-2142.Cont
CRL-2142.SARS
CRL-2149.Cont
CRL-2149.SARS
CRL2271.Cont
CRL2271.SARS
CRL-127.Cont
CRL-127.SARS

Figure 1

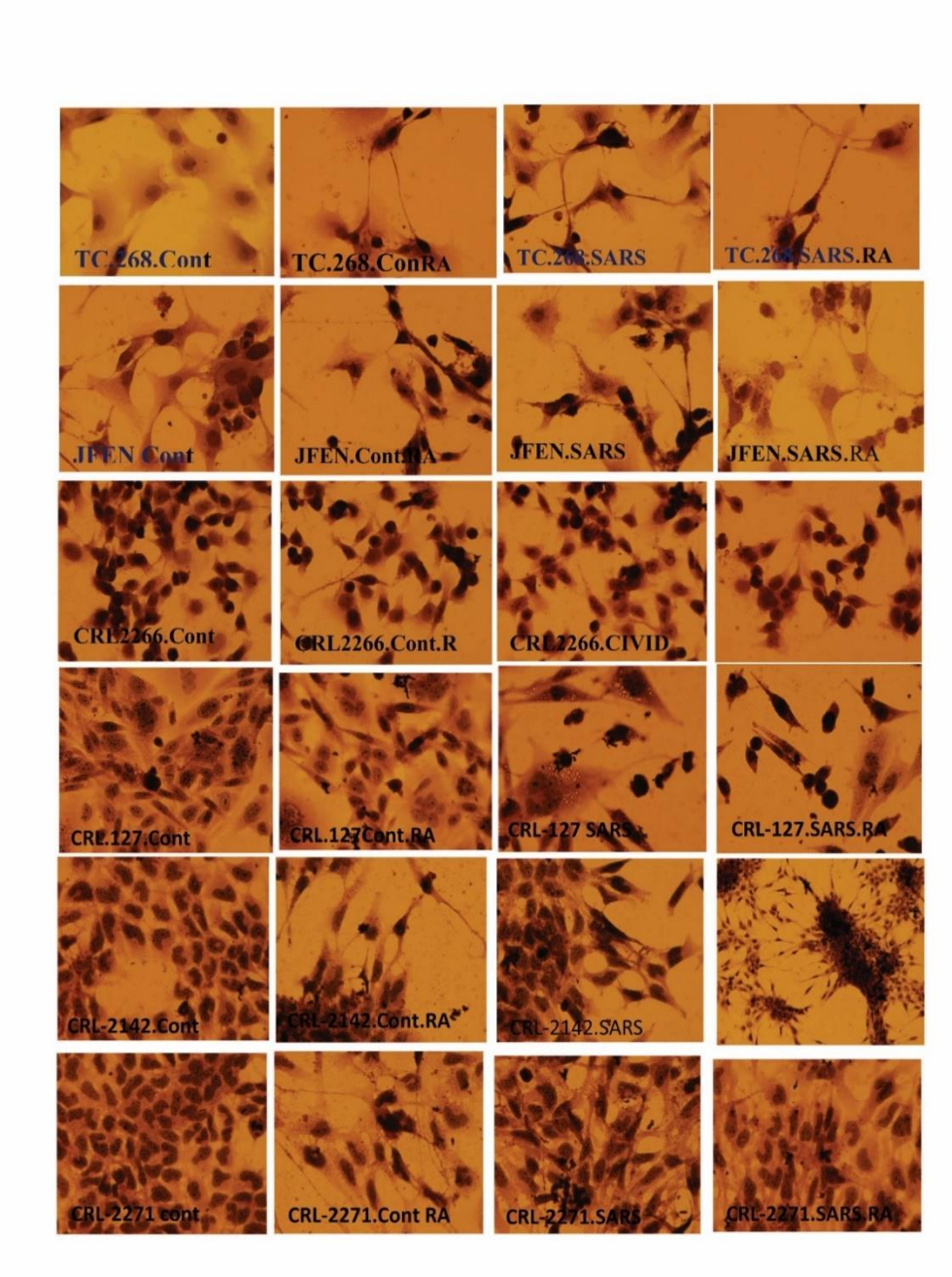
TC.268.Cont
TC.268.ConRA
TC.268.SARS
TC.268.SARS.RA
JFEN Cont
JFEN.Cont.RA
JFEN.SARS
JFEN.SARS.RA
CRL2266.Cont
CRL2266.Cont.R
CRL2266.CIVID
CRL.127.Cont
CRL.127Cont.RA
CRL-127 SARS
CRL-127.SARS.RA
CRL-2142.Cont
CRL-2142.Cont.RA
CRL-2142.SARS
CRL-2271 cont
CRL-2271.Cont RA
CRL-2271.SARS
CRL-2271.SARS.RA

Figure 2

Morphological Study: All the human developing neuronal cell lines, infected as well as uninfected controls, were observed once a day post-infection. Cytopathic effects (CPE) were discernable within 72 hours post-infection in TC-268 and JFEN, when the neurons began to exhibit clustering foci on the monolayers. The numbers of foci increased on days 4 and 5. On the upper surface of the foci, rounded cells appeared that formed syncytia-like structures; these were apparently dead cells. The CPE were more prominent in the TC-268 cell line when compared to JFEN. JFEN showed rapid thinning of the monolayer instead of CPE and infection with SARS-COV-2 produced acute lytic effects in JFEN rather than the CPE described for the TC-268. Both infected cell lines also exhibited neurite deformations, exhibiting highly abnormal morphology, including neurons showing elongation of cells, vacuolation within the cytoplasm, enlargement of the neuronal cell body, shortening, thinning or abnormal increase in axonal length, change in cellular diameter, and central chromatolysis, and other aberrant cellular morphology (Fig. 2). None of the other six cell lines showed any morphologic changes and appeared to be nonpermissive to the cytopathic effects of SARS-COV-2. Therefore, even 12 weeks post-infection, the cells grew at a similar rate to uninfected cells. However, RA induced noticeable morphologic changes to all eight cell lines. RA induced immediate CPE in TC-268 and JFEN and stimulated the process of differentiation in the rest of the non-permissive cell lines, with elongations of axonal length as well as elongations of neurons. CRL-127 exhibited amplification of neuronal vacuoles and development of unusually large neurons. CRL-127 was the only cell line that became permissive to SARS-CoV-2 (Table 1 and Fig. 2) Immunostaining with SARS-CoV-2 Ab, as well as RT-qPCR, confirmed the relative permissiveness of CRL-127 to SARS-COV-2

(Table 1; Fig. 2). In addition, after RA-treatment, CRL-127 was positive for the TMPRS22 receptor.

In summary, RA-treatment induced partial differentiation in all six non-permissive cell lines and CRL-127 became permissive to SARS-COV-2 infection. RA also induced marked and significant changes of the neurons and caused neurite deformation, enlargement of the neuronal cell body, shortening or abnormal increase and thinning of axonal length, vacuole formation, and selective neurotoxicity.

Discussion

Since January 2020 SARS-CoV-2 outbreaks have been documented around the globe. The speed at which the pandemic spread has emphasized inherent deficiencies in national emergency preparedness and response protocols for most countries. Mounting evidence points to SARS-CoV-2 being highly contagious and easily transmittable via droplets and fomites and it has been mostly associated with ARDS in hospitalized patients (Rothan and Byareddy, 2020). Anosmia and hypogeusia, the inability or decreased ability to smell and taste, have been reported as common and specific symptoms in the SARS-CoV-2 infected. Most of the latter show no other symptoms and regain their smell and taste (Altin et al., 2020; Meng et al., 2020). The study of Lechien et al (5), who recruited 417 mild to moderate COVID-19 patients from 12 European hospitals, reported that 85.6% and 88.0% of patients described olfactory and gustatory dysfunctions, respectively and that a significant association existed between both disorders ($p < 0.001$). Olfactory dysfunction (OD) appeared before other symptoms in 11.8% of cases. There are numerous reports describing anosmia with incident rates varying between 41% to 80%$^{+}$, depending on populations studied (Klinger et al., 2020; Mehraeen et al., 2020). Nevertheless, the severity of smell dysfunction varies

widely among patients (Moein et al., 2020) with many illustrating a reduction in taste and chemesthetic sensing (Parma et al., 2020).

One objective of the present study was to explore whether brain neurons, that are constantly going through neurogenesis, were primary targets of SARS-CoV-2. Neurogenesis in the adult human brain has been confirmed in two regions *viz.* the subventricular zone (SVZ) of the anterior lateral ventricles - the site of origin for olfactory bulb neurons, and the dentate gyrus (DG) of the hippocampus, the region of a human brain that is involved in learning and memory. In the SVZ, progenitor cells migrate to the olfactory bulb, where they terminally differentiate into neurons and serve the role of sensing odors. In contrast, DG cells divide along the sub-granular zone and migrate into the granule cell layer before terminally differentiating into granule cells. Since none of the progenitor neuronal cell lines were permissive to the SARS-CoV-2 virus, it is unlikely that they represent targets of SARS-CoV-2. However, upon RA-induced differentiation, one cell line, CRL-127, expressed a low degree of permissiveness to the virus.

Our studies also examined the entry mechanism of the virus. RT-PCR and immunofluorescence assay positive presence of the virus were correlated with the degree of expression of serine protease, TMPRSS2. The SARS-CoV-2 comprises four main structural proteins *viz.* spike (S), envelope (E) and membrane glycoproteins and a nucleocapsid (N) protein. The S is a transmembrane protein located on the viral surface and enables binding of E proteins to host cells by attraction to angiotensin-converting enzyme 2 [ACE2] (Walls et al., 2020). The S glycoprotein comprises two subunits: S_1, which binds to the host cell receptor and S_2 which fuses the viral and host cell's membranes (Tortorici and Vessler, 2019; Walls et al., 2020). After fusion, type II transmembrane serine protease (TMPRSS2) cleaves

the ACE-2 and activates the S proteins to facilitate virus entry into the host cell (Rabi et al., 2020). Without TMPRSS2 the virus can not enter the cell which has prompted some to suggest that TMPRSS2 might represent an intervention point for SARS-CoV-2 treatment (Rahmann et al., 2020; Hoffmann et al., 2020). We also observed low expression of ACE2 for all the neuronal cell lines utilized in this investigation. However, none of the neuronal cell lines expressing low *ACE2* were permissive to SARS-CoV-2. We believe that this may be due to the absence of ACE2 protein on the neuronal surface or that permissiveness may require minimal *ACE2* receptor density on the cellular surface for the entry of the virus. This notion may require further study.

The importance of *ACE2* receptors has been thoroughly investigated, but without the engagement of *TMPRSS2*, the virus cannot enter target cells.

In some studies, the investigators did not identify ACE2 receptors and this absence of ACE2 receptors, with the clear evidence of olfactory neuronal damage, is explained by indirect entry of COVID-19 (Brann et al 2020.). However, recent data by Klingenstein et al [2021] have shown expressions of both ACE2 and *TMPRSS2*. They showed *ACE2* is located in the sustentacular cells and in the glandular cells in the olfactory epithelium as well as in the basal cells, glandular cells, and epithelial cells of the respiratory epithelium. They also showed *TMPRSS2* in the sustentacular cells and the glandular cells of the olfactory epithelium, providing clear evidence for the basic anatomical evidence for the expression of ACE2 and TMPRSS2 in the human nose, olfactory epithelium, and olfactory bulb. Fodoulian et al [2021] have also shown substantial expression of the genes coding for the virus receptor *ACE2* and for the *TMPRSS2, which act as a* virus internalization enhancer. They carried out a human olfactory single-cell RNA-seq dataset and determined that sustentacular cells, which

maintain the integrity of olfactory sensory neurons, express *ACE2* and *TMPRSS2*. *ACE2* protein was highly expressed in a subset of sustentacular cells in human and mouse olfactory tissues. In addition to some contradictions regarding the presence or absence of *ACE2* receptors on olfactory neurons, it should be noted that an overwhelming body of evidence conform the infection of olfactory neurons including the duration of loss of smell (anosmia or dystonia) in a significant number of patients, evidence of changes within the olfactory bulb on MRI imaging, identification of viral particles within the olfactory bulb in post-mortem specimens and the inverse association between severity of COVID-19 and the prevalence of olfactory loss [Hopkins et al 2021]. Recent study by Altunisik et al [2021] have described expressions of *ACE2* receptors on glial cells neurons, skeleton muscle cells. They have reported several post-COVID-19 manifestations including neurological symptoms in 31.37 % patients [the most common neurological symptom was headache in ~20%of the patients [].

It should be noted that we have analyzed the permissiveness of SARS-CoV-2 *in vitro*. *In vivo* the olfaction is a very complex process, and the OB is a multilayer structure where odor information is relayed to the CNS in the sequential stages, and the TCs, OB glomeruli and MCs interact in a highly coordinated fashion. In our experimental model we tested a monolayer of olfactory neuronal cell lines. Therefore, no precise mechanisms can be discerned. Humans have between 10 and 20 million olfactory receptor neurons. It is unlikely that all of olfactory neurons will die immediately after COVID-19 in every infected individual. As shown by Altunisik et al [2021] that a small number of infected individuals suffer from complete anosmia. Butowt and von Bartheld [2020] have described that there is significant difference in the prevalence of loss of smell in patients in different populations

[Butowt & Bartheld 2020]. For example, they showed that in East Asian anosmia prevalence is ~22%, where as in Western countries it is 48% [Butowt & Bartheld 2020]. Variations in spike protein in SARS-CoV-2 also plays an important role since not all variants are expected to have the same affinity for *ACE2*. The replication rate of the viral variations in other proteins in the virus also plays an important role since all the virus variants are not replicating as the same rate. And, finally, the initial viral load may all impact on the loss of smell. These authors have noted that olfactory neurons do not express *ACE2* receptors which is now clearly refuted by the more recent reports [Altunisik et al., 2021; Fodoulian et al 2021; Klingenstein et al 2021]. They argue that if SARS-CoV-2 is cytopathic to olfactory neurons then why some individuals regain their sense of smell quickly and others take long time. However, no one has clearly shown that all the olfactory neurons are killed by the virus. The genetic variations in the spike proteins and *ACE2* variations within the *ACE2* receptors and the complex-six layered structure may play an important role in protecting the OB from complete destruction. Also, olfaction is a highly complex process involving six-layers just in OB and we are not aware if *ACE2* receptors are expressed in all six-layers of olfactory neurons. They argue that the replacement of olfactory neurons takes 8 to 10 days and additional 5 days for cilia maturation, but the recovery of smell in SARS-CoV-2 takes about a week. This suggests that the COVID-19 infection does not necessarily kills all of the olfactory neurons but, cytopathic effects on OB most likely injures a small part of neurons in OB. It should be noted that we are unaware at what stage of differentiation olfactory neurons express ACE2 receptors. If this occurs at the terminal stage of differentiation that it would explain why some people regain their smell after a week since it will take only 3-5 days for the cilia to recover. There are still many unknowns in the mystery of anosmia and

dysnomia. For example, we do not know if the organization of odorant sensory neurons [OSNs] is affected. The axons of OSNs expressing the same odorant receptors converge onto the same glomerulus at the OB throughout the adult neurogenesis. Does the SARS-CoV-2 infection disturb the precise locations of convergence after viral induced cytopathic effects?

As mentioned above that a significant numbers of COVID-19 infected patients exhibit several post-COVID-19 adverse effects, including muscle pain, fatigue, memory loss and headache [Hopkins et al 2021; Hu et al 2020Pellegrini et al., 2020;Uversky et al 2021]. We wanted to know if neuronal differentiation plays any role in increasing the permissiveness of the virus. Therefore, RA-induced differentiations was carried out to address this particular question. Our results suggest that in the majority of the cell lines partial differentiation does not appear to play any role in increasing the permissiveness of the virus. Only in one cell line (i.e., CRL-127) we found slight upregulation of ACE2. However, our results remain inconclusive regarding answering this question.

Even though several reports describe severe neurological impacts of COVID-19 patients (Asadi-Pooya and Simani, 2020; Baig, 2020; Wu et al., 2020), our current understanding of how the virus disseminates and migrates into the CNS remains incomplete. Recent animal models have, however, shed some light on the probable route for viral invasion of the CNS. The mouse *ACE2* structure is different from the human ACE2 but a transgenic mouse model, where human *ACE2* coding sequences were introduced into wild-type mice, under control of the human cytokeratin 18 (K18) promoter, has revealed interesting results. When K18-hACE2 transgenic mice were infected with SARS-CoV, the infection rapidly spread to the alveoli and then, remarkably, spread to subcortical and cortical regions of the mouse brain,

via the olfactory route (McCray et al., 2020). This model suggests the main entry of SARS-CoV to the CNS is via the olfactory bulb (Netland et al., 2008) and this has been elegantly demonstrated for SARS-CoV infections in ACE2 transgenic mice (Natoli et al., 2020). The limitation of the present study is that we have utilized olfactory cell lines rather than human subjects (which, of course, would be unethical). We have only used two olfactory neuronal cell lines and a geographically restricted viral strain. While there are infinite differences between the *in vivo* human brain and olfactory bulb and the *in vitro* state as presented herein, despite this limitation, we believe that a clear picture of permissiveness of olfactory neurons is demonstrated, without a gender bias, and suggests a prospective mechanism for SARS-CoV-2-based anosmia.

References cited

Altin, F., Cingi, C., Uzun, T., Bal, C. (2020). Olfactory and gustatory abnormalities in COVID-19 cases. Eur Arch Otorhinolaryngol 7, doi: 10.1007/s00405-020-06155-9.

Altunisik E, H S Sayiner, S Aksoz, E Cil, G Ozgenc. Neurological symptoms in COVID-19 patients
Bratisl Lek Listy. 2021;122(1):39-44. doi: 10.4149/BLL_2021_004.

Asadi-Pooya, A.A., Simani, L. (2020). Central nervous system manifestations of COVID-19: A systematic review. J Neuro Sci 413, 116832.

Baig, A.M. (2020). Neurological manifestations in COVID-19 caused by SARS-CoV-2. CNS Neurosci Ther 26, 499-501.

Bilinska, K., Butowt, R. (2020). Anosmia in COVID-19: A bumpy road to establishing a cellular mechanism. ACS Chem Neurosci 11, 2152-2155.

Boillat [M], C Kan, V Pauli et al, Non-neuronal expression of SARS-CoV-2 entry genes in the olfactory system suggests mechanisms underlying COVID-19-associated anosmia. Sci Adv. 2020 Jul 31;6(31):eabc5801. doi: 10.1126/sciadv.abc5801.

Brann DH , T Tsukahara , C Weinreb et al, Non-neuronal expression of SARS-CoV-2 entry genes in the olfactory system suggests mechanisms underlying COVID-19-associated anosmia. Sci Adv. 2020 Jul 31;6(31):eabc5801. doi: 10.1126/sciadv.abc5801.

Burgos-Blasco, B., Güemes-Villahoz, N., Donate-Lopez, J., Vidal-Villegas, B., García-Feijóo, J. (2020). Optic nerve analysis in COVID-19 patients. J Med Virol 10.1002/jmv.26290. doi:10.1002/jmv.26290.

Butowt R, C S von Bartheld. Anosmia in COVID-19: Underlying Mechanisms and Assessment of an Olfactory Route to Brain Infection Neuroscientist. 2020 Sep 11;1073858420956905. doi: 10.1177/1073858420956905.

CDC (2020). Interim laboratory biosafety guidelines for handling and processing specimens associated with coronavirus disease 2019 (COVID-19). https://www.cdc.gov/coronavirus/2019-ncov/lab/lab-biosafety-guidelines.html. Accessed June 2020.

CDC (2021). Symptoms of coronavirus. http://www.cdc.gov/coronavirus/2019-ncov/symptoms-testing/symptoms.html accessed 01/22/2021.

Coronaviridae Study Group of the International Committee on Taxonomy of Viruses (2020). The species *Severe acute respiratory syndrome-related coronavirus*: classifying 2019-nCoV and naming it SARS-CoV-2. Nature Microbiol 5, 536-544.

Fodoulian L , J Tuberosa , D Rossier et al. SARS-CoV-2 Receptors and Entry Genes Are Expressed in the Human Olfactory Neuroepithelium and Brain iScience. 2020 Dec 18;23(12):101839. doi: 10.1016/j.isci.2020.101839.

Hoffmann, M., Kleine-Weber, H., Schroeder, S., Kruger, N., Herrler, T., et al. (2020). SARS-CoV-2 cell entry depends on ACE2 and TMPRSS2 and is blocked by a clinically proven protease inhibitor. Cell 181, 271-280.

Hu J, J Jolkkonen , C Zhao Neurotropism of SARS-CoV-2 and its neuropathological alterations: Similarities with other coronaviruses. Neurosci Biobehav Rev. 2020 Dec;119:184-193. doi: 10.1016/j.neubiorev.2020.10.012.

Hughes, B.W., Addanki, K.C., Sriskanda, A., McLean, E., Bagasra, O. (2016). Infectivity of immature neurons to Zika virus: A link to congenital Zika syndrome. eBioMedicine 10, 66-70.

Johnson, N.P., Mueller, J. (2002). Updating the accounts: global mortality of the 1918–1920 “Spanish” influenza pandemic. Bull Hist Med 76, 105-115.

Hopkins C, J R Lechien, S Saussez. More than ACE2? NRP1 may play a central role in the underlying pathophysiological mechanism of olfactory dysfunction in COVID-19 and its association with enhanced survival Med Hypotheses. 2021 Jan;146:110406. doi: 10.1016/j.mehy.2020.110406.

Klinger, V.T., Tenório Lins Carnaúba, A., Wanderley Rocha, K., Cristina Lyra de Andrade, K., Ferreira, S.M.S., Menezes, P. Olfactory and taste disorders in COVID-19: A systematic review. Braz J Otorhinolaryngol 9 doi: 10.1016/j.bjorl.2020.05.008.

Klingenstein M, S Klingenstein , P H Neckel , A F Mack , A P Wagner , A Kleger , S Liebau , A Milazzo

Evidence of SARS-CoV2 Entry Protein ACE2 in the Human Nose and Olfactory Bulb Cells Tissues

Organs. 2021 Jan 22;1-10. doi: 10.1159/000513040.

Klopfenstein, T., Kadiane-Oussou, N.J., Toko, L., Royer, P.Y., Lepiller, Q., Gendrin, V. (2020). Features of anosmia in COVID-19. Med Mal Infect https://doi.org/10.1016/j.medmal.2020.04.006.

Lechien, J.R., Chiesa-Estomba, C.M., Siati, D.R., Horoi, M., Le Bon, S.D., *et al*. (2020). Olfactory and gustatory dysfunctions as a clinical presentation of mild-to-moderate forms of the coronavirus disease (COVID-19): a multicenter European study. Eur Arch Oto-Rhino-Lar 277, 2251-2261.

McCray, P.B., Pewe, L., Wohlford-Lenane, C., Hickey, M., Manzel, L., et al. (2007). Lethal infection of K18-hACE2 mice infected with severe acute respiratory syndrome coronavirus. J Virol 81, 813-821.

Mehraeen, E., Behnezhad, F., Salehi, M.A., Noori, T., Harandi, H., Alinaghi, S.A.S. (2020). Olfactory and gustatory dysfunctions die to the coronavirus disease (COVID-19): A review of current evidence. Eur Arch Otorhinolaryngol 1–6. doi: 10.1007/s00405-020-06120-6.

Meng, X., Deng, Y., Dai, Z., Meng, Z. (2020). COVID-19 and anosmia: A review based on up-to-date knowledge. Am J Otolaryngol 41, 102581.

Moein, S.T., Hashemian, S.M., Mansourafshar, B., Khorram-Tousi, A., Tabarsi, P., Doty, R.L. (2020). Smell dysfunction: a biomarker for COVID-19. Int For Aller Rhinol 10, 944-950.

Netland, J., Meyerholz, D.K., Moore, S., Cassell, M., Perlman, S. (2008). Severe acute respiratory syndrome coronavirus infection causes neuronal death in the absence of encephalitis in mice transgenic for human ACE2. J Virol 82, 7264-7275.

Parma, V., Ohla, K., Veldhuizen, M.G., Niv, M.Y., Kelly, C.E., et al. (2020). More than smell—COVID-19 is associated with severe impairment of smell, taste, and chemesthesis, Chem Sen 45, 609-622.

Pellegrini L , A Albecka, D L Mallery et al SARS-CoV-2 Infects the Brain Choroid Plexus and Disrupts the Blood-CSF Barrier in Human Brain Organoids. Cell Stem Cell. 2020 Dec 3;27(6):951-961.e5. doi: 10.1016/j.stem.2020.10.001.

Rabi, F.A., Al Zoubi, M.S., Kasasbeh, G.A., Salameh,. D.M., Al-Nasser, A.D. (2020). SARS-CoV-2 and coronavirus disease 2019: what we know so far. Pathogens 9, 231.

Rahman, N., Basharat, Z., Yousuf, M., Castaldo, G., Rastrelli, L., Khan, H. (2020). Virtual screening of natural products against type II transmembrane serine protease (TMPRSS2), the priming agent of coronavirus 2 (SARS-CoV-2). Molecules 25, 2271.

Rothan, H.A., Byrareddy, S.N. (2020). The epidemiology and pathogenesis of coronavirus disease (COVID-19) outbreak. J Autoimmun 109, 102433.

Spinney, L. (2018). Pale rider: the Spanish flu of 1918 and how it changed the world. Johnathan Cape, London, UK.

Spreeuwenberg, P., Kroneman, M., Paget, J. (2018). Reassessing the global mortality burden of the 1918 influenza pandemic. Am J Epidemiol 187, 2561-2567.

Tortorici, M.A., Veesler, D. (2019). Structural insights into coronavirus entry. Adv Virus Res 105, 93-116.

Vaira, L.A., Salzano, G., Deiana, G., De Riu, G. (2020). Anosmia and ageusia: Common findings in COVID-19 patients. Laryngoscope, 130, 1787. https://doi.org/10.1002/lary.28692.

Uversky V N, F Elrashdy , A Aljadawi et al. Severe acute respiratory syndrome coronavirus 2 infection reaches the human nervous system: How? J Neurosci Res. 2021 Mar;99(3):750-777. doi: 10.1002/jnr.24752. Epub 2020 Nov 20.

Walls, A.C., Park, Y.J., Tortorici, M.A., Wall, A., McGuire, A.T., Veesler, D. (2020). Structure, Function, and Antigenicity of the SARS-CoV-2 Spike Glycoprotein. Cell 181, 281-292.

Wu, Y., Xu, X., Chen, Z., Duan, J., Hashimoto, K., Yang, L., Liu, C., Yang, C. (2020). Nervous system involvement after infection with COVID-19 and other coronaviruses. Brain Beh Imm 87, 18-22